Herschel-SPIRE: Design, Ground Test Results, and Predicted Performance

Matt Griffin[*,a], Bruce Swinyard[b], Laurent Vigroux[c], Alain Abergel[d], Peter Ade[a], Philippe André[e], Jean-Paul Baluteau[f], James Bock[g], Alberto Franceschini[h], Walter Gear[a], Jason Glenn[i], Maohai Huang[j], Douglas Griffin[b], Ken King[b], Emmanuel Lellouch[k], David Naylor[l], Seb Oliver[m], Göran Olofsson[n], Ismael Perez-Fournon[o], Mat Page[p], Michael Rowan-Robinson[q], Paolo Saraceno[r], Eric Sawyer[b], Gillian Wright[s], Annie Zavagno[f], Asier Abreu[b], George Bendo[q], Alan Dowell[b], Darren Dowell[g], Marc Ferlet[b], Trevor Fulton[t], Peter Hargrave[a], Glenn Laurent[i], Sarah Leeks[b,u], Tanya Lim[b], Nanyao Lu[u], Hien Nguyen[g], Alan Pearce[b], Edward Polehampton[b,l], Davide Rizzo[q], Bernhard Schulz[u], Sunil Sidher[b], Dave Smith[b], Locke Spencer[l], Ivan Valtchanov[v], Adam Woodcraft[s], Kevin Xu[u], Lijun Zhang[u], and the SPIRE Consortium.

[a] School of Physics and Astronomy, Cardiff University, 5 The Parade, Cardiff CF24 3YB, UK
[b] Rutherford Appleton Laboratory, Oxfordshire, UK
[c] Institut d'Astrophysique de Paris, France
[d] Institut d'Astrophysique Spatiale, Orsay, France
[e] Service d'Astrophysique, CEA, Saclay, France
[f] Observatoire de Marseille, France
[g] Jet Propulsion Laboratory, Pasadena, California, USA
[h] Università di Padova, Italy
[i] University of Colorado, Boulder, Colorado, USA
[j] National Astronomical Observatories of China, Beijing, China
[k] Observatoire de Paris, France
[l] University of Lethbridge, Lethbridge, Alberta, Canada
[m] University of Sussex, UK
[n] Stockholm Observatory, Sweden
[o] Instituto de Astrofísica de Canarias, Tenerife, Spain
[p] Mullard Space Science Laboratory, Surrey, UK
[q] Imperial College, University of London, UK
[r] Istituto di Fisica dello Spazio Interplanetario, Rome, Italy
[s] UK Astronomy Technology Centre, Edinburgh, UK
[t] Blue Sky Spectroscopy, Lethbridge, Alberta, Canada
[u] Infrared Processing and Analysis Center, Pasadena, California, USA
[v] ESA Herschel Science Centre, ESAC, Villafranca, Spain

ABSTRACT

SPIRE, the Spectral and Photometric Imaging Receiver, is a submillimetre camera and spectrometer for Herschel. It comprises a three-band camera operating at 250, 350 and 500 μm, and an imaging Fourier Transform Spectrometer covering 194-672 μm. The photometer field of view is 4x8 arcmin., viewed simultaneously in the three bands. The FTS has an approximately circular field of view of 2.6 arcmin. diameter and spectral resolution adjustable between 0.04 and 2 cm^{-1} ($\lambda/\Delta\lambda$ =20-1000 at 250 μm). Following successful testing in a dedicated facility designed to simulate the in-flight operational conditions, SPIRE has been integrated in the Herschel spacecraft and is now undergoing system-level testing prior to launch. The main design features of SPIRE are reviewed, the key results of instrument testing are outlined, and a summary of the predicted in-flight performance is given.

Keywords: Herschel, Far Infrared, Submillimetre, Instrumentation

* E-mail: matt.griffin@astro.cf.ac.uk; Telephone: +44-(0)29-2087-4203; Fax: +44-(0)29-2087-4056

Space Telescopes and Instrumentation 2008: Optical, Infrared, and Millimeter,
edited by Jacobus M. Oschmann, Jr., Mattheus W. M. de Graauw, Howard A. MacEwen,
Proc. of SPIE Vol. 7010, 701006, (2008) · 0277-786X/08/$18 · doi: 10.1117/12.788312

1. INTRODUCTION

The European Space Agency's Herschel Space Observatory[1] is scheduled for launch at the end of 2008. Its main scientific goals are the statistics and physics of galaxy and structure formation at high redshift and the study of the early stages of star formation. These scientific investigations require deep imaging surveys at far-infrared (FIR) and submillimetre wavelengths, and photometry and spectroscopy of individual sources. SPIRE is designed to exploit the particular advantages of Herschel: its large-aperture (3.5 m), cold, (~ 80 K), low-emissivity (< 2%) telescope; unrestricted access to the poorly explored 200-700-μm range; and the large amount of high quality observing time. Although the instrument design is dictated by Herschel's main science themes, it will offer a powerful tool for many other astrophysical studies: giant planets, comets, the galactic interstellar medium, nearby galaxies, ultraluminous infrared galaxies, and active galactic nuclei. Its capabilities will remain unchallenged by the ground-based and the airborne observatories which are planned to come into operation over the next decade.

2. INSTRUMENT OVERVIEW

SPIRE contains a three-band imaging photometer and an imaging Fourier Transform Spectrometer (FTS), both of which use bolometer arrays operating at 0.3 K. The photometer field of view is 4 x 8 arcmin., the largest that could be achieved given the location of the SPIRE field of view in the Herschel focal plane and the size of the telescope unvignetted field of view. Three bolometer arrays are used for broad-band photometry ($\lambda/\Delta\lambda \sim 3$) in spectral bands centred on approximately 250, 350 and 500 μm. The same field of view is observed simultaneously in the three bands through the use of two fixed dichroic beam-splitters. Signal modulation can be provided either by SPIRE's two-axis Beam Steering Mirror (BSM) or by scanning the telescope across the sky. An internal thermal source is available to provide a repeatable calibration signal for the detectors. The FTS has spatially separated input and output ports. One input views a 2.6-arcminute diameter field of view on the sky and the other is fed by an on-board reference source. Two bolometer arrays at the output ports are sensitive in overlapping bands providing complete wavelength coverage between 194 and 672 μm. The FTS spectral resolution is set by the total optical path difference, and can be adjusted between 0.04 and 2 cm^{-1} (corresponding to $\lambda/\Delta\lambda = 1000 - 20$ at 250 μm). The lowest spectral resolution that is planned to be used for spectrophotometric observations is 1 cm^{-1}.

The photometer and spectrometer both have cold pupil stops conjugate with the Herschel secondary mirror, which is the system pupil for the telescope and defines a 3.29-m diameter used portion of the primary. Feedhorns provide a roughly Gaussian illumination of the pupil, with an edge taper of around 8 dB in the case of the photometer arrays.

The SPIRE focal plane unit (FPU) is approximately 700 x 400 x 400 mm in size and is supported from the 10-K cryostat optical bench by thermally insulating mounts. The FPU has three temperature stages: the Herschel cryostat provides temperatures of 4.5 K and 1.7 K via high thermal conductance straps to the instrument, and an internal ^{3}He refrigerator cools all five detector arrays to approximately 0.3 K. Two sets of JFET preamplifiers are used to read out the bolometer signals, one for the photometer and one for the spectrometer. The JFET units are attached to the 10-K optical bench next to the 4.5-K enclosure, with the JFETs heated internally to their optimum operating temperature of ~ 120 K.

There are three SPIRE warm electronics units: the Detector Control Unit (DCU) provides the bias and signal conditioning for the arrays and cold electronics, and demodulates and digitises the detector signals; the FPU Control Unit (FCU) controls the ^{3}He cooler and the two FPU mechanisms, and reads out all the FPU thermometers; and the Digital Processing Unit (DPU) runs the on-board software interfaces with the spacecraft for commanding and telemetry. The 130 kbs available data rate allows all photometer or spectrometer detectors to be sampled and the data transmitted to the ground with no on-board processing.

3. THREE-BAND IMAGING PHOTOMETER

3.1 Optical design and layout of the photometer

Optics: Figure 1 shows the layout of the photometer. The photometer optical design[2] is all-reflective except for the dichroics used to direct the three bands onto the bolometer arrays, and the filters used to define the passbands. The image is diffraction-limited over the 4 x 8 arcmin. field of view, which is offset by 11 arcmin. from the centre of the Herschel telescope's highly curved focal surface. The 4.5-K optics are mounted on the SPIRE internal optical bench. (The input

optics are common to the photometer and spectrometer and the separate spectrometer field of view is directed to the other side of the optical bench panel by a pick-off mirror.) The 1.7-K enclosure contains the detector arrays, dichroics and fold mirrors. The bolometer array modules of the photometer are bolted to the outside wall of the 1.7-K box. Inside each one, the ^{3}He stage, accommodating the detectors, feedhorns and final filters, is thermally isolated from by tensioned Kevlar threads, and cooled by a thermal strap to the ^{3}He cooler.

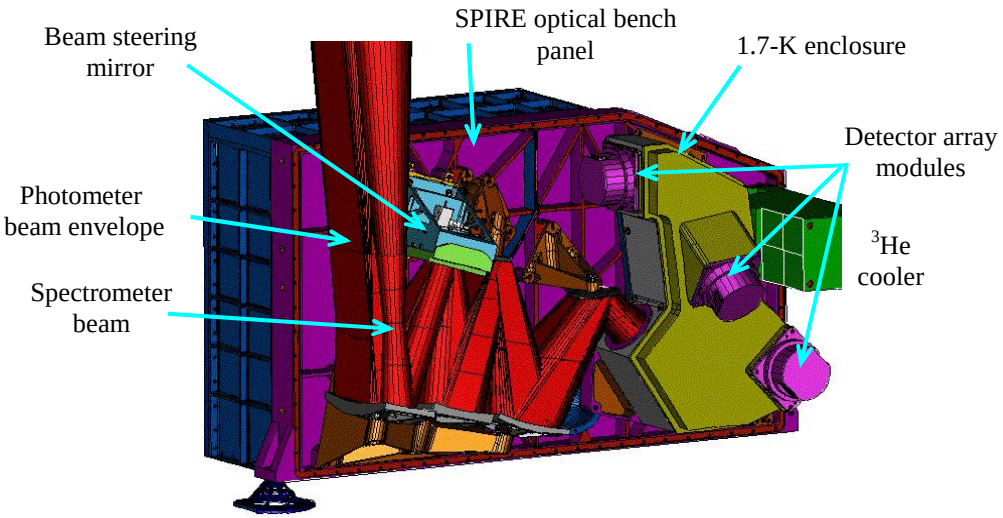

Figure 1: Computer-generated image of the SPIRE photometer layout.

Beam steering mirror: The beam steering mirror[3] (BSM) can chop ± 2 arcmin. along the long axis of the 4 x 8 arcmin. field of view, at a nominal frequency of 2 Hz. It can simultaneously chop at up to 1 Hz in the orthogonal direction by up to 30". This two-axis motion allows "jiggling" of the pointing to create a fully sampled image of the sky with the feedhorn-coupled detectors whose diffraction-limited beams on the sky are separated by approximately twice the beam FWHM.

Internal calibration source: An internal thermal source[4,5] provides a repeatable signal for the bolometers. It radiates through a hole in the centre of the BSM, occupying an area contained within the region of the pupil obscured by the hole in the primary. The source can produce a power at the detector of a few x 10^{-14} W, 1-2% of the telescope background. With a detector NEP of a few x 10^{-17} W Hz$^{-1/2}$, this gives a large instantaneous S/N.

Filters and dichroics: Quasi-optical filters[6] define the bands with high out-of-band rejection, and minimise the thermal load on the low-temperature stages by reflecting short-wavelength radiation. The bands are defined by a combination of transmission edges (of filters in front of the detectors), reflection/transmission edges of the dichroics, and the cutoff wavelengths of the feedhorn output waveguides.

Bolometer arrays: The SPIRE detectors[7-10] are spider-web bolometers using NTD germanium thermometers, which are coupled to the telescope by hexagonally close-packed $2F\lambda$-diameter single-mode conical feedhorns, giving diffraction limited beams of FWHM 19, 24 and 35" for the 250, 350 and 500-μm bands respectively. The three arrays contain 43 (520 μm), 88 (360 μm) and 139 (250 μm) detectors. The array layouts are shown schematically in Figure 2(a) and Figure 2(b) is a photograph of an array module. Each unit has an identical interface to the 1.7-K box and a thermal strap from the ^{3}He cooler to the 0.3-K stage, which is supported by Kevlar cords from the 1.7-K level. The bolometers are AC-biased with frequency adjustable over the range 50 - 300 Hz, reducing $1/f$ noise from the JFET readout, and giving a $1/f$ knee for the system of less than 50 mHz.

3.2 Observing modes for the imaging photometer

The photometer will have three principal observing modes, as illustrated in Fig. 4 and described below. More details can be found in the SPIRE Observer's Manual[11].

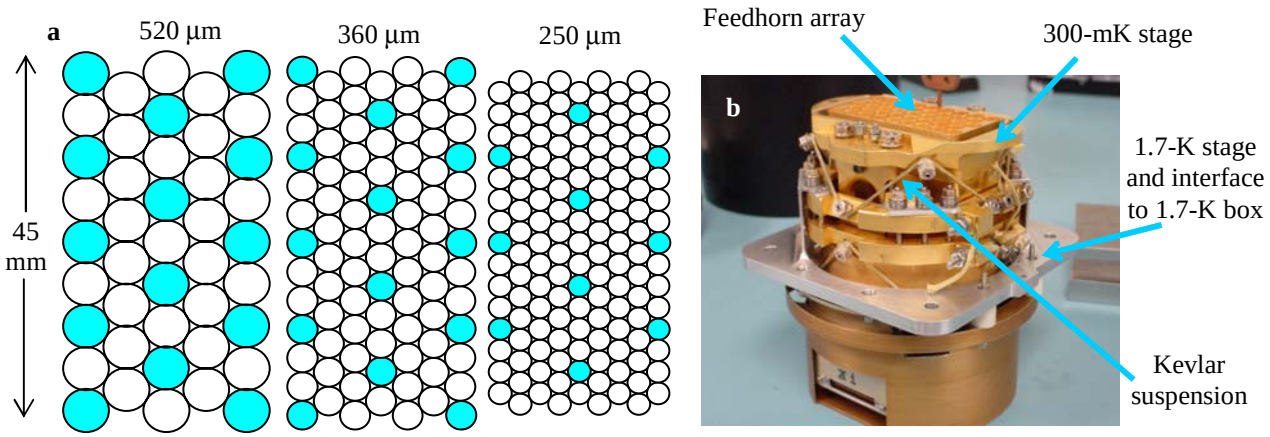

Figure 2: (a) Layout of the photometer arrays. The shaded detectors are those for which there is exact overlap on the sky for the three bands; (b) SPIRE PLW detector array module.

Point or compact source photometry: Several sets of three detectors have beams at the three wavelengths that are co-aligned on the sky (shaded circles in Figure 2). By chopping through an angle of 126", three-band photometry can be carried out with maximum efficiency: the source is observed in one of the detectors in each band at all times. The standard observing mode for point sources will use the beam steering mirror to make a seven-point map in which the nominal position and six hexagonally arranged neighbouring positions are observed in turn. With an angular offset of 6", the S/N loss for a given integration time is about 20% in the worst case (250 µm band). This is a small price to pay for assurance that pointing or source position errors do not result in flux density errors. The data from all detectors in all of the arrays will also be transmitted to the ground, providing sparsely sampled maps of the field around the object.

Field (jiggle) mapping: For mapping of regions a few arcmin. in size, the beam steering mirror will perform a jiggle map, similar to the mode of operation of the SCUBA bolometer camera on the JCMT[12]. A 64-point jiggle pattern is needed to achieve full spatial sampling in all bands simultaneously, with a step size of 9" (half-beam spacing at 250 µm). The 250-µm band image will be critically sampled, and the other two will be oversampled. A maximum field size of 4 x 4 arcmin. is available in this mode as the 2-arcmin. regions at each end of the array will be chopped outside the field of view admitted by the photometer optics.

Scan mapping: This mode will be used for maps bigger than the SPIRE field of view, including deep surveys. The telescope will be scanned across the sky at up to 1 arcmin. s^{-1}. The nominal scan rate is currently taken to be 30" s^{-1}. To give the beam overlap needed for full spatial sampling over a strip defined by one scan line, and to provide a uniform distribution of integration time over the area covered by the scan, the scan angle is tilted with respect to the array axes, and cross-scanning ins implemented on order to minimise the effect of 1/*f* drifts.

4. IMAGING FOURIER TRANSFORM SPECTROMETER

4.1 Optical design and layout of the spectrometer

The FTS[13-14] uses two broadband intensity beam splitters in a Mach-Zehnder configuration. All four ports of the interferometer are independently accessible as in the Martin-Puplett (M-P) polarising FTS. But the throughput is a factor of two higher than for the M-P as none of the incoming radiation is rejected, and there is no sensitivity to the polarisation of the incident radiation. A thermal source at the second input port allows the background power from the telescope to be matched. The amplitude of the interferogram central maximum is proportional to the difference in the radiant power from the two ports, so this allows the large telescope background to be nulled, reducing the dynamic range requirements for the detector sampling. Detector arrays are placed in the two output ports to accommodate the 194 – 672 µm range in two with overlapping bands. A single back-to-back scanning roof-top mirror serves both interferometer arms. It has a frictionless mechanism using double parallelogram linkage and flex pivots, and a Moiré fringe sensing system.

FTS optics and filters: The layout of the FTS is shown in Figure 3. The spectrometer beam enters through a hole in the panel into the FTS side of the instrument. A pupil stop is located between the pick-off mirror and the input fold mirror. It is brought to an intermediate focus just after the first beam divider, after which the it is collimated and sent to a moving roof-top mirror. The roof-top shifts the beam and sends it towards the camera mirror, which produces an image just before an output beam divider. The beam is then focused onto the detector arrays which are located inside the 1.7-K enclosure. Each array has a lens incorporated in its 0.3-K filter stack to correct for the non-telecentric FTS optics and provide more uniform fringe contrast and efficiency across the field.

Filters: A filtering scheme similar to the one employed for the photometer channel is used to restrict the passband of the instrument. The bands cover 194-324 μm (SSW) and 316-672 μm (SLW), overlapping at the 90% level.

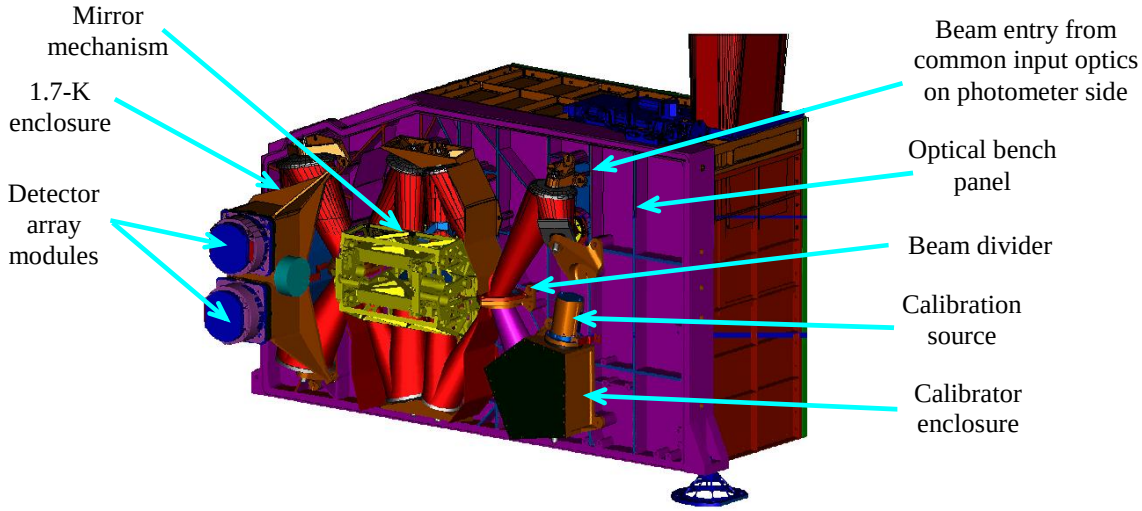

Figure 3: Computer-generated image of the SPIRE FTS layout.

FTS detector arrays: The two spectrometer arrays contain 37 hexagonally close-packed detectors in the short-wavelength array and 19 in the long-wavelength array. The array modules are similar to those used for the photometer, with an identical interface to the 1.7-K enclosure. The layout of the FTS arrays is shown schematically in Figure 4. The detectors on the periphery are partly vignetted by the 2.6-arcminute field of view admitted by the instrument optics (shown by the large circles in Figure 4). The feedhorn and detector cavity designs are carefully optimised to provide good sensitivity across the whole wavelength range of the FTS. The SSW feedhorns are sized to give $2F\lambda$ pixels at 225 μm and the SLW horns are $2F\lambda$ at 389 μm. This arrangement has the advantage that there are many co-aligned pixels in the combined field of view. The SSW beams on the sky are 27" apart, and the SLW beams are separated by 48". The beam widths are expected to be approx. 16" for the SSW band and 35" for SLW.

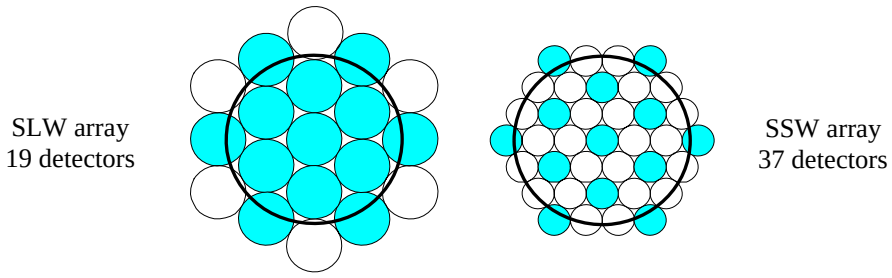

Figure 4: Spectrometer detector arrays. The shaded detectors are co-aligned on the sky in the two bands.

4.2 FTS operating modes and spectral resolution

The nominal FTS operating mode involves continuous scanning of the mirror while the detectors are sampled. The beam steering mechanism is stationary and the scan mirror is moved (nominally at 0.5 mm s^{-1}, giving an optical path rate of 2 mm s^{-1} due to the factor of four folding in the optics). Radiation frequencies of interest are encoded as detector output electrical frequencies in the range 3-10 Hz. The maximum scan length is 3.5 cm, corresponding to an optical path difference of 14 cm. To ensure that mechanism jitter noise is well below the photon noise level, the mirror position has a relative accuracy of 0.1 μm. The need to null the strong telescope background means that the FTS calibration source has to be on continuously. As a back-up mode, a step-and-integrate scheme can be implemented, in which the scan mirror is placed in turn at a set of positions to form a scan, with the BSM providing signal modulation at each step. The FTS spectral resolution can be adjusted between 0.04 and 2 cm^{-1} ($\lambda/\Delta\lambda$ = 1000-20 at 250 μm), by setting the scan length. The instrumental line shape is a sinc function, and the unapodised spectral resolution, $\Delta\sigma$, is the distance from the peak of the sinc function to its first zero crossing point. The standard observing modes use three different spectral resolutions: low ($\Delta\sigma$ = 1 cm^{-1}); medium (0.25 cm^{-1}) and high (0.04 cm^{-1}). The corresponding resolving powers $\lambda/\Delta\lambda = \sigma/\Delta\sigma$ for the three cases are shown in Figure 5 as a function of wavelength.

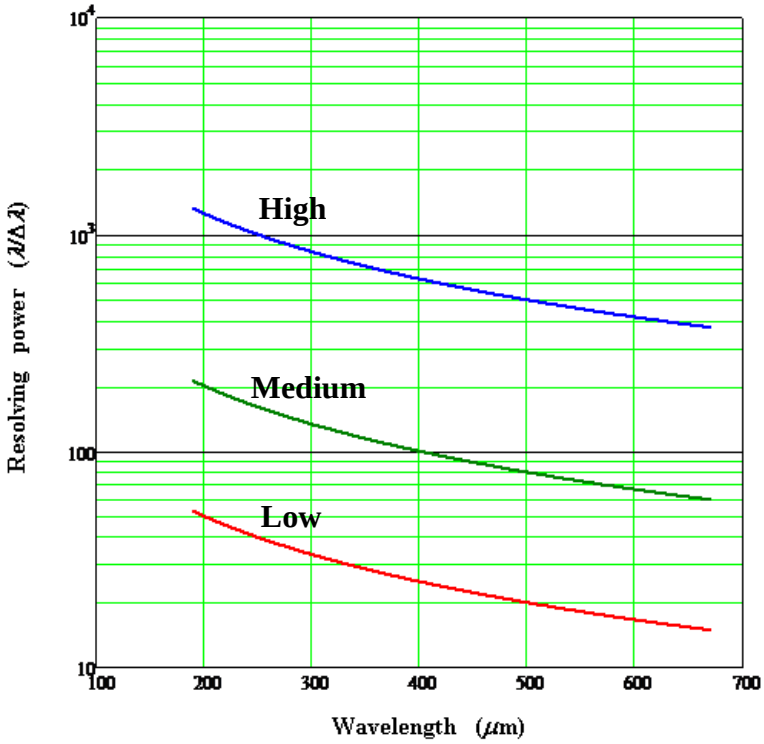

Figure 5: FTS unapodised resolving power vs. wavelength for the standard settings (High, Medium, Low).

For point sources, the object will be positioned at the centre of the array, but data will be acquired for all of the detectors, providing at the same time a sparsely-sampled map of the emission from the region around the source. Likewise, a single pointing will give a sparsely-sampled map of an extended object. For fully-sampled spectral mapping, the beam steering mirror will provide the necessary pointing changes between scans. Further details of the FTS observing modes are given in the SPIRE Observers' Manual[11].

5. ^{3}HE COOLER AND 300-MK THERMAL STRAP SYSTEM

The same ^{3}He cooler design[15] is be used for both the SPIRE and PACS instruments. Gas gap heat switches control the cooler and there are no moving parts. Liquid confinement in zero-*g* is achieved by a porous material which holds the liquid by capillary attraction. A Kevlar wire suspension supports the cooler during launch whilst minimising the

parasitic heat load. The cooler contains 6 STP litres of ^{3}He, fits in a 200 x 100 x 100-mm envelope and weighs about 1.7 kg. Operating from 1.7 K, it achieves a temperature of 274 mK with a 10-μW load and a 46 hr hold time, and a total time-averaged power load on the 1.7 K heat sink of ~ 3 mW. Copper straps connect the 0.3-K stage to the five detector arrays, and are held rigidly at various points by Kevlar support modules[16]. The supports at the entries to the 1.7-K boxes are also designed to be light-tight. The cooler will be recycled during periods when the Herschel telemetry antenna is pointed towards Earth for data downlink and command uplink. In these ~ 3-hr periods, operation of the instruments is not planned due to possible interference from the transponder operation and the highly restricted pointing.

6. INSTRUMENT TEST RESULTS

The SPIRE flight model (FM) has been assembled, tested and calibrated at the Rutherford Appleton Laboratory in the UK. The custom-built test facility[17] has a large cryostat to house the FPU and to replicate the temperatures of the Herschel optical bench and the 1.7-K and 4.5-K stages. By means of a flip mirror, the instrument can be made to view either a large-area temperature-controlled cryogenic black body filling its beam, or it can view external sources through the cryostat window. The radiant background is set by the temperature of the cryogenic black body or by a set of cold neutral density filters when viewing outside the cryostat. A telescope simulator allows the optical characteristics of the Herschel telescope to be reproduced, and an external Fourier transform spectrometer has been installed to allow the instrument spectral response to be measured. A hot black body and a far infrared laser are available as external sources for tests requiring continuum and monochromatic input beams.

Five cooldown campaigns were carried out during the FM build, with the last two performed on the final FPU incorporating all flight hardware. The FPU has also been successfully subjected to cold vibration at the Herschel cryo-vibration facility at the Centre Spatial de Liège.

300-mK system: The ^{3}He cooler performs within specification, achieving a cold tip temperature of less than 290 mK. In the final FPU, the hold time has been measured at 64 hrs with a 1.55 K interface temperature, somewhat colder than the value expected in flight (1.74 K). Thermal modelling predicts that the hold time requirement of 46 hrs will be met in flight with nominal interface temperatures and heat load.

Detectors: The instrument-level performance of the detector arrays is described in detail by Schulz et al.[18]. The dark noise performance is within 15% of ideal bolometer model predictions. An empirical method to correct temperature dependent long term signal variations has been successfully implemented, and the corrected signals show no evidence of a $1/f$ knee above 50 mHz. The end-end detector channel yield (including detector, JFETs, harness and electronics) is high, with only two photometer channels and one spectrometer channel inoperative, and highly uniform sensitivity levels across the arrays. The thermal and electrical properties of the detectors can be very accurately modelled using ideal bolometer theory[19,20]; the results of such modelling are presented by Woodcraft et al.[21]

Optics: The photometer and FTS optical characteristics have been extensively evaluated and found to be in excellent agreement with the instrument design. Based on measurements made with the facility telescope simulator, the predicted beam sizes have been determined. The photometer beams have FWHM of (19, 24, 35)" for the (250, 250, 500) μm bands, in close agreement with predictions. For the FTS, the multi-moded behaviour of the feedhorns means that modelling of the beams is not straightforward. Based on analysis of instrument test results, the predicted SSW FWHM varies between 15.5" and 17" from the centre to the band edges. Pending confirmation in flight, a value of 16" has been adopted for the whole band. For SLW, the FWHM varies between approximately 32" and 40" from the centre to the band edges. Pending in-flight confirmation, a value of 35" has been adopted for the whole band. The measured optical performance is described in detail by Ferlet et al.[22].

Filters and passbands: The overall passbands have been characterised using the external FTS, and the results are in good agreement with expectations. Figure 6a shows the average spectral pass-bands for the photometer compared with the filter profiles constructed from the individual filter component measurements and modelled nominal waveguide responses. The original positions of one the dichroic measured edges had to be shifted slightly to achieve agreement with the measured data. This is attributed to the off-axis incidence of the beam in the instrument. The three bands are centred at approximately 250, 350 and 500 μm, with $\lambda/\Delta\lambda$ of 3.3, 3.4, and 2.5 respectively. The longest wavelength band is slightly wider than the design value, and the medium-wavelength band slightly narrower, but these differences have minimal impact on the sensitivity or scientific optimisation of the bands. The measured FTS bands for the central

detectors are shown in Figure 6b, compared with the stacked filter passbands.

Overall instrument transmission: The overall transmission of the instrument has been evaluated from bolometer load curves measured with the instrument viewing a variable temperature cryogenic black body at the entrance aperture, and comparing the results with values expected from a model of the instrument transmission that takes into account the passband profiles and expected transmissions, the detector optical efficiencies (measured at array level), and losses due to the optics. The results are summarised in Table 1, and are in agreement to 20% in the worst case. A similar assessment of the FTS transmission shows good agreement between the measured and expected transmission of 20%.

Array	250 µm	350 µm	500 µm
Measured transmission	0.38	0.36	0.37
Predicted transmission	0.30	0.34	0.29

Table 1: Measured and predicted overall instrument transmission for the photometer (averaged over each array)

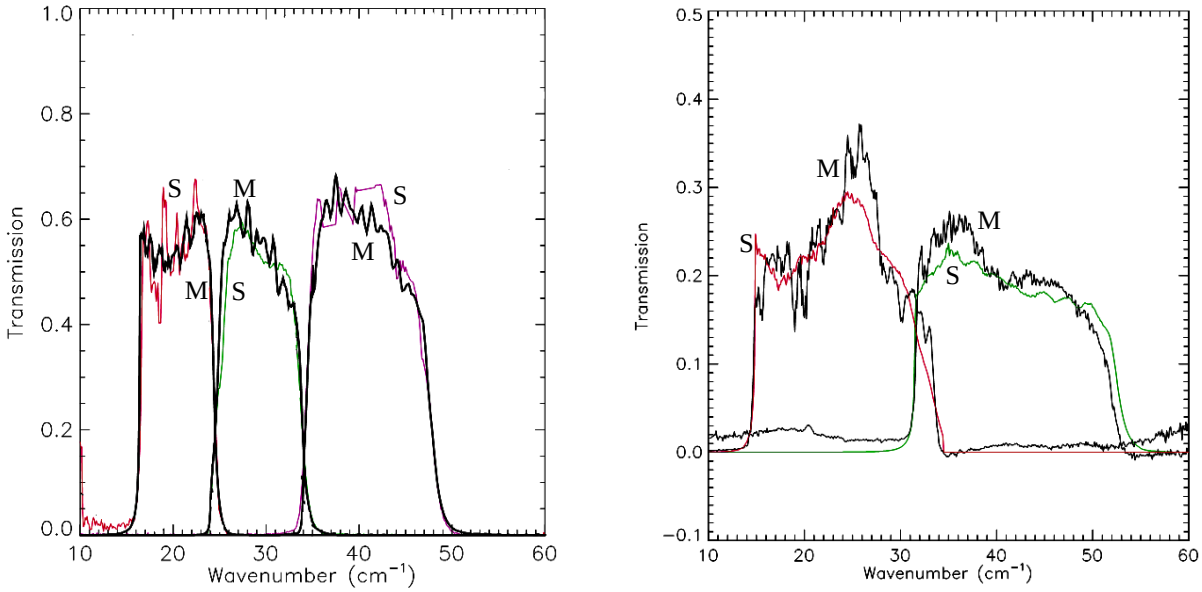

Figure 6: (a) Average spectral passbands for the photometer as measured (M) and derived by stacking transmissions of individual components (S); (b) similar plots for the two spectrometer bands. The measured curves are normalised to the same peak values as the stacked profiles.

Spectrometer performance: The performance of the FTS has been fully characterised during the instrument level test, and is within specification in all important respects (passbands and overlap, maximum and minimum spectral resolution, fringe contrast, dead time, and velocity control. A detailed assessment of the FTS performance is given by Spencer et al. [23].

Internal calibrators: The photometer internal calibrator (PCal) performs nominally, providing a fast, high S/N signal for both the photometer and FTS detectors. The FTS calibrator (SCal) has been used successfully to null background signals over the range expected from the telescope. The main purpose of SCal is to null the large central maximum due to the telescope background. It has been decided to leave a small residual central maximum in order to establish the zero path difference to high accuracy. One minor shortcoming of SCal as implemented is that it was originally designed to be

able to cope with a 4% emissive telescope, whereas the effective emissivity is now expected to be on the order of only 1% over the SPIRE range. This is very beneficial for the instrument sensitivity, but a consequence is that the telescope spectrum cannot nulled as uniformly as was planned over the entire range. However, instrument tests have demonstrated that this effect can be removed in the FTS processing[24] .

Beam Steering Mechanism: The BSM has been shown to meet or exceed all operational and performance requirements, including angular range, position holding, and settling time. Meeting the settling time requirement of 20 ms can prove difficult, requiring careful tuning of the servo parameters. However, the system response is dominated by the low-pass filter in the detector signal analogue chain[25], so a minor non-compliance in BSM settling time will have negligible impact on the data.

Warm electronics: The flight analogue and digital electronics perform as designed and within specification.

On-Board Software: The SPIRE on-board software has been comprehensively tested and de-bugged in the course of instrument testing.

Outstanding technical issues: A the time of writing, some aspects of in-flight performance remain to be fully demonstrated, and will be the subject of specific tests and analyses during Herschel system level testing prior to launch. These include:

(i) The detectors have been observed to be susceptible to high levels of electromagnetic interference in the 30-MHz range if the disturbance is modulated at low frequencies. Tests to date show that the actual levels radiated by the Herschel spacecraft are orders of magnitude lower than the levels that showed a problem in testing, and are not likely to be modulated at the audio frequencies. Further system level tests are planned to confirm this.

(ii) Possible susceptibility of the spectrometer mechanism position measurement system to microphonic disturbance from the spacecraft reaction wheels is still to be evaluated at system level, but this is not foreseen to be a major problem since the microphonic environment in the instrument test facility was likely more extreme than in flight.

(iii) An increase of ~ 25 mK in the temperature drop between the cooler cold tip and the detector arrays was observed to occur after instrument-level vibration. The reason for this is unclear, and attempts to reproduce it in vibration and thermal cycling of representative hardware have shown no evidence of such an effect. A possible further increase at system level could produce a degradation in detector sensitivity.

In summary, although various problems and anomalies remain to be addressed, as is typical for the first operation of such a complex system, most performance requirements have already been demonstrated, as have many of the goals.

7. INSTRUMENT PERFORMANCE ESTIMATES

The sensitivity of SPIRE has been estimated using photometric models which have been largely verified by instrument level testing. The models are similar to those used in the 2006 SPIE paper on SPIRE[26], but have been updated to take into account new information from instrument tests and a lower estimate of the telescope emissivity (now typ. 1% across the SPIRE range compared with the 4% previously assumed) based on Herschel reflector emissivity measurements[27] and stray light modelling by the industrial contractor. The updated models predict somewhat better sensitivity levels than before, and have been used to provide the input data for HSpot[28] (the Herschel observation preparation tool provided by the Herschel Science Centre), which also calculates instrument and telescope overheads.

Photometer: For a point source observation, the shortest available observation of total duration 580 s (256 s on-source integration time, 143 s instrument overheads; 180 s telescope overheads) yields rms noise levels of 1.6 mJy or less in all bands. Longer observations are more efficient in terms of overheads, but may not be necessary in most cases as the extragalactic confusion limit is expected to be in the region of 7 mJy rms[29,30]. For the shortest feasible 4 x 4 arcmin. jiggle map, with total duration 687 s (256 s on-source integration time, 251 s instrument overheads; 180 s telescope overheads), the corresponding point source sensitivity is 6.3 mJy rms or less in all bands, again reaching the expected confusion limit. For mapping regions larger than 4 x 4 arcmin., the standard observing mode is scan mapping, which is especially efficient for large areas. Although the achievable sensitivity depends on the details of the observation, particularly the map size, it is illustrated by the case of 0.5 x 0.5 deg. map of duration 1175 s (944 s on-source

integration time, 651 s instrument overheads; 180 s telescope overheads), attaining rms sensitivities of (10, 13, 11) mJy at (250, 350, 500) μm.

Spectrometer: For point source line spectroscopy ($\Delta\sigma$ = 0.04 cm^{-1}), a typical observation of 1372 s duration s (1066 s on-source integration time, 126 s instrument overheads; 180 s telescope overheads) yields rms line flux sensitivity limits between 0.8 and 1.5 x 10^{-17} W m^{-2} depending on the wavelength. Shorter observations are possible, but less efficient. For low-resolution spectrophotometry ($\Delta\sigma$ = 1 cm^{-1}), a typical observation of 844 s duration s (512 s on-source integration time, 192 s instrument overheads; 180 s telescope overheads) results in rms flux density limits between 37 and 70 mJy depending on the wavelength.

Further details are given in the SPIRE Observer's Manual[11], and HSpot[28] can be used to estimate the sensitivity for a given observation. Prior to launch, the instrument performance levels that are used in the current version of HSpot will be updated to reflect the latest instrument knowledge from instrument and system level tests, but will not change significantly. It should be noted that, as with many cryogenic infrared space instruments, predicted sensitivity figures are subject to large uncertainties (at least a factor of two) due to uncertainties the instrument performance in flight and, in the case of SPIRE, the effective telescope background.

8. DATA PROCESSING

All SPIRE observations will be processed by pipelines operating fully automatically, which shall produce standard calibrated data products (maps, point source fluxes, maps, spectral data cubes, etc.). It will also be possible for users to run the pipelines interactively in order to modify parameters and assumptions if desired. The standard data processing pipeline for the photometer, is described by Griffin et al.[25] and that for the spectrometer by Fulton et al.[24]. Software simulators[31,32] have been developed to model the behaviour of the photometer and FTS and produce realistic data streams that will allow instrument operating modes to be optimised and data reduction software to be evaluated.

9. THE SPIRE CONSORTIUM

Besides the Co-Investigators and project team members listed as the authors of this paper, many people have contributed to the technical development of SPIRE including: Jean-Louis Augueres, Chris Brockley-Blatt, Martin Caldwell, Christophe Cara, Goutam Chattopadhyay, Riccardo Cerulli, John Coker, Patrick Collins, Dustin Crumb, Colin Cunningham, Pascal Dargent, Gary Davis, Peter Davis-Imhof, John Delderfield, Iris Didschuns, Anna Di Giorgio, Kjetil Dohlen, Lionel Duband, Roger Emery, Didier Ferrand, Peg Frerking, Steve Guest, Anneso Goizel, Martin Harwit, Vic Haynes, Marty Herman, Viktor Hristov, Len Husted, Don Jennings, Dean Jocelin, Brian Kiernan, Andrew Lange, Jerry Lilienthal, John Lindner, Francoise Loubere, Bruno Maffei, Jerome Martignac, Karine Mercier, Guy Michel, Sergio Molinari, Harvey Moseley, Anthony Murphy, Jim Newell, Renato Orfei, Ian Pain, Gary Parks, Phil Parr-Burman, Frederic Pinsard, Giampaolo Pisano, Dominique Pouliquen, Faiz Rahman, Tony Richards, Louis Rodriguez, Samuel Ronayette, Brooks Rownd, Dominique Schmitt, Srinivasan Sethuraman, Bruce Sibthorpe, Brian Stobie, Rashmi Sudiwala, Kalyani Sukhatme, Carole Tucker, Anthony Turner, Tim Waskett, Mark Weilert, Berend Winter.

REFERENCES

1. G. Pilbratt, "Herschel mission overview and key programmes", in *Space Telescopes and Instrumentation I: Optical, Infrared, and Millimeter Wave*, Marseille, 23-28 June 2008, *Proc. SPIE* 7010-01 (this volume).
2. K. Dohlen, A. Orignéa, D. Pouliquen, and B. Swinyard, "Optical design of the SPIRE instrument for FIRST", *Proc. SPIE* 4013, 119, 2000.
3. I. Pain, B. Stobie, G.S. Wright, T. A. Paul, and C.R. Cunningham, "SPIRE beam steering mirror: a cryogenic two-axis mechanism for the Herschel Space Observatory", *IR Space Telescope and Instruments, Proc. SPIE* 4850, 619, 2003.
4. G. Pisano, P. Hargrave, M. Griffin, P. Collins, J. Beeman, and R. Hermoso, "Thermal illuminators for far-infrared and submillimeter astronomical instruments", *Applied Optics IP*, 44 (16), 3208, 2005.

5. P. Hargrave, T. J. Waskett, T. L. Lim, and B.M. Swinyard, "Performance of flight-model on-board calibration sources on Herschel-SPIRE", in *Millimeter and Submillimeter Detectors and Instrumentation for Astronomy III, ,* Orlando, 27-31 May 2006, *Proc. SPIE* 6275, 2006.
6. P.A.R. Ade, G. Pisano, C.E. Tucker, and S.O. Weaver, *A review of metal mesh filters,* In *Millimeter and Submillimeter Detectors and Instrumentation for Astronomy III, ,* Orlando, 27-31 May 2006, *Proc. SPIE* 6275.
7. A.D. Turner, J.J. Bock, H.T. Nguyen, S. Sethuramam, J.W. Beeman, J. Glenn, P.C. Hargrave, A.L. Woodcraft, V.V. Hristov, and F. Rahman, "Si_3N_4 micromesh bolometer array for sub-millimeter astrophysics". *Applied Optics* 40, 4921, 2001.
8. B. Rownd, J.J. Bock, G. Chattopadhyay, J. Glenn, and M. Griffin, "Design and performance of feedhorn-coupled arrays coupled to submillimeter bolometers for the SPIRE instrument aboard the Herschel Space Observatory". *Proc. SPIE* 4855, 510-519, 2003.
9. G. Chattopadhyay, J.J. Bock, K. Rownd, M. Caldwell, and M. J. Griffin, "Feed horn coupled bolometer arrays for SPIRE – design, simulations and measurements", *IEEE. Trans. Microwave Theory and Techniques*, 51, 2139, 2003.
10. H.T. Nguyen. "A report of the laboratory performance of the flight bolometric detector arrays for SPIRE/Herschel", in *Millimeter and Submillimeter Detectors and Instrumentation for Astronomy III, ,* Orlando, 27-31 May 2006, *Proc. SPIE* 6275, 2006.
11. "SPIRE Observers' Manual", HERSCHEL-HSC-DOC-0789 (http://herschel.esac.esa.int/Documentation.shtml)
12. W.S. Holland, E.I. Robson, W. K. Gear, C.R. Cunningham, J.F. Lightfoot, T. Jenness, R.J. Ivison, J.A. Stevens, P.A.R. Ade, M.J. Griffin, W.D. Duncan, J.A. Murphy, and D.A. Naylor, "SCUBA: a common-user submillimetre camera operating on the James Clerk Maxwell Telescope", *Mon. Not. R. Astron. Soc.* 303, 659, 1999.
13. B.M. Swinyard, K. Dohlen, D. Ferrand, J.-P. Baluteau, D. Pouliquen, P. Dargent, G. Michel, J. Martignac, P. Ade, P. Hargrave, M. Griffin, D. Jennings, and M. Caldwell, "Imaging FTS for Herschel-SPIRE". *Proc. SPIE* 4850, 698, 1993.
14. P.A.R Ade, P.A. Hamilton, and D.A. Naylor, "An absolute dual beam emission spectrometer", *Fourier transform spectroscopy: new methods and applications*, OSA, 90, 1999.
15. L. Duband, "Spaceborne helium adsorption coolers", Proceedings of ESA Symposium on *The Far Infrared and Submillimetre Universe*, Grenoble, 15-17 April 1997, *ESA SP-401*, 357, 1997.
16. P. Hargrave, J.J. Bock, C. Brockley-Blatt, J. Coker, L. Duband, A. Goizel, D.K. Griffin, and B.M. Swinyard, "The 300 mK system for Herschel-SPIRE", in *Millimeter and Submillimeter Detectors and Instrumentation for Astronomy III, ,* Orlando, 27-31 May 2006, *Proc. SPIE* 6275, 2006.
17. P.A. Collins, D.L. Smith, M. Ferlet, T. Grundy, M. Harman, M.J. Griffin, P.A.R. Ade, and B.M. Swinyard, *Ground calibration facility for Herschel-SPIRE*. *Proc. SPIE* 4850, 628-637, 2003.
18. B. Schulz, J.J. Bock, N. Lu, H.T. Nguyen, C.K. Xu, L. Zhang, C.D. Dowell, M.J. Griffin, G.T. Laurent, T.L. Lim, and B.M. Swinyard, "Noise Performance of the Herschel-SPIRE Bolometers during instrument ground tests", in *Millimeter and Submillimeter Detectors and Instrumentation for Astronomy*, Marseille, 23-28 June 2008, *Proc. SPIE* 7020-74.
19. J.C. Mather, "Bolometer noise, nonequilibrium theory", Applied Optics, 21, 1125, 1982.
20. R.V. Sudiwala, M.J. Griffin, and A.L. Woodcraft, "Thermal modelling and characterisation of semiconductor bolometers", *Int. Journal of Infrared and Mm Waves*, 23, 545, 2002.
21. A.L. Woodcraft, H.T. Nguyen, J. J. Bock, B. Schulz, B.M. Swinyard, and M. Griffin, "Understanding the Herschel-SPIRE bolometers", in *Millimeter and Submillimeter Detectors and Instrumentation for Astronomy*, Marseille, 23-28 June 2008, *Proc. SPIE* 7020-14.
22. M.J. Ferlet, G. Laurent, B.M. Swinyard, J. Glenn, J.J. Bock, and K. Dohlen, "Characterization of Herschel/SPIRE flight model optical performances", in *Space Telescopes and Instrumentation I: Optical, Infrared, and Millimeter Wave*, Marseille, 23-28 June 2008, *Proc. SPIE* 7010-103 (this volume).
23. L.D. Spencer, B. Zhang, D. A. Naylor, P. Davis-Imhof, T.R. Fulton, J-P Baluteau, M.J. Ferlet, T.L. Lim, E.T. Polehampton, and B.M. Swinyard, "Performance evaluation of the Herschel/SPIRE instrument flight model-imaging Fourier transform spectrometer", in *Space Telescopes and Instrumentation I: Optical, Infrared, and Millimeter Wave*, Marseille, 23-28 June 2008, *Proc. SPIE* 7010-07 (this volume).
24. T.R. Fulton, D.A. Naylor, J.-P. Baluteau, M. Griffin, P. Davis-Imhof, B.M. Swinyard, T. Lim, C. Ordenovic, C. Surace, D. Clements, P. Panuzzo, R. Gastaud, E.T. Polehampton, and S. Guest, "The data processing pipeline for the Herschel/SPIRE imaging Fourier transform spectrometer", ", in *Space Telescopes and Instrumentation I: Optical, Infrared, and Millimeter Wave*, Marseille, 23-28 June 2008, *Proc. SPIE* 7010-102 (this volume).

25. M.J. Griffin, C. D. Dowell, T. Lim, G. Bendo, J.J. Bock, N. Castro-Rodriguez, D. Clements, P. Chanial, R. Gastaud, J. Glenn, K.J. King, G. Laurent, N. Lu, G. Mainetti, H. Morris, H.T. Nguyen, P. Panuzzo, D. Rizzo, B. Schulz, A. Schwartz, B.M. Swinyard, K. Xu, and L. Zhang, "The SPIRE photometer data-processing pipeline", in *Space Telescopes and Instrumentation I: Optical, Infrared, and Millimeter Wave*, Marseille, 23-28 June 2008, *Proc. SPIE* 7010-99 (this volume).
26. M. Griffin, A. Abergel, P. Ade, P. André, J.-P. Baluteau, J. Bock, A. Franceschini, W. Gear, J. Glenn, D. Griffin, K. King, E. Lellouch, D. Naylor, G. Olofsson, I. Perez-Fournon, M. Rowan-Robinson, P. Saraceno, E. Sawyer, A. Smith, B. Swinyard, L. Vigroux, and G. Wright, "Herschel-SPIRE: design, performance, and scientific capabilities", *Space Telescopes and Instrumentation I: Optical, Infrared, and Millimeter*. *Proc. SPIE*, 6265, 62650A, 2006.
27. J. Fischer, T. Klassen, N. Hovenier, G. Jakob, A. Poglitsch, and O. Sternberg, "Cryogenic far-infrared laser absorptivity measurements of the Herschel Space Observatory telescope mirror coatings", *Applied Optics*, 43, 3765, 2004.
28. "HSpot Users' Guide" (http://herschel.esac.esa.int/Docs/HSPOT/pdf/hspot_om.pdf)
29. M. Vaccari, "Extragalactic confusion limits in Herschel Key Programmes", in: Proc. *Studying Galaxy Evolution with Spitzer and Herschel*, Crete, May 28–June 2, 2006, Charmandaris, V., Rigopoulou, D., Kylafis, N. (Eds.), Crete University Press Conference Series (in press).
30. M. Vaccari, "EG Confusion Limits in Herschel KPs", herschel.esac.esa.int/OT_KP_wkshop/pops/FEB21/02.Vaccari.pdf
31. B. Sibthorpe, A.L. Woodcraft, and M.J. Griffin, "A software simulator for the Herschel-SPIRE imaging photometer", *Proc. SPIE* 5487, 2004.
32. J. V. Lindner, D.A. Naylor, and B.M. Swinyard. "SHIFTS: a simulator for the Herschel imaging Fourier transform spectrometer", in *Space Telescopes and Instrumentation I: Optical, Infrared, and Millimeter*, Orlando, 24-31 May 2006, *Proc. SPIE* 6265, 62652-Y, 2006.